ISSN: 1692-7257 - Volume 1 – Number 47 - 2026

RCTA
Revista Colombiana de Tecnologías de Avanzada
UNIPAMPLONA

Digital Object Identifier: 10.24054/rcta.v1i47.4295

Experimental assessment of a Gorlov hydrokinetic microturbine for rural low-flow use

Evaluación experimental de una microturbina hidrocinética Gorlov para uso rural de bajo caudal

MSc. Jorge Enrique Meneses Flórez [1], Ing. Kevin Alexander Ramírez Rodríguez [1], Ing. Henry David Méndez Chávez [1]

*[1] **Universidad Industrial de Santander (UIS),** Escuela de Ingeniería Mecánica, Grupo de Investigación en Conectividad y Procesado de Señales - CPS, Bucaramanga, Santander, Colombia.*

***Correspondence:** jmeneses@uis.edu.co*

***Received:** August 10, 2025. **Accepted:** December 20, 2025. **Published:** January 01, 2026.*

***How to cite:** J. E. Meneses Flórez, K. A. Ramírez Rodríguez, y H. D. Méndez Chávez, "Evaluación experimental de una microturbina hidrocinética Gorlov para uso rural de bajo caudal", RCTA, vol. 1, n.º. 47, pp. 99-108, Jan. 2026. Recovered from https://ojs.unipamplona.edu.co/index.php/rcta/article/view/4295*

Abstract: This study develops and evaluates a Gorlov-type hydrokinetic microturbine for electricity generation in low-flow rivers in rural Colombia. A river in Santander was hydraulically characterized, and a NACA 0015 rotor was designed and 3D-printed. Experimental tests delivered 3.3 W of power and 8.8 % efficiency, with a 40 % increase in extracted energy when channeling the flow through a 2.5 m pipe. The stable rotor behavior and gearbox-based transmission confirm its technical and educational feasibility as a low-cost renewable solution for decentralized electrification.

Keywords: hydrokinetic microturbine, Gorlov rotor, additive manufacturing, rural electrification.

Resumen: El estudio desarrolla y evalúa una microturbina hidrocinética tipo Gorlov para generar electricidad en ríos de bajo caudal en zonas rurales de Colombia. Se caracterizó hidráulicamente un cauce en Santander y se diseñó un rotor NACA 0015 fabricado por impresión 3D. Las pruebas experimentales registraron 3.3 W de potencia y 8.8 % de eficiencia, aumentando 40 % la energía captada mediante canalización del flujo con una tubería de 2.5 m. El desempeño estable del rotor y la transmisión por caja de engranajes validan su viabilidad técnica y educativa como alternativa renovable de bajo costo para electrificación descentralizada.

Palabras clave: microturbina hidrocinética, rotor Gorlov, manufactura aditiva, electrificación rural.

1. INTRODUCTION

Electricity supply in rural areas of Colombia faces historical challenges, despite the fact that 70% of energy comes from large hydroelectric plants with high environmental and social impact [1]. The UPME [2] points out that more than 500,000 people in non-interconnected areas lack continuous access to electricity or depend on fossil fuels, limiting development. Distributed generation solutions

based on micro renewable sources offer a sustainable way to address this problem. Specifically, free-flow hydraulic microturbines (hydrokinetic systems) are a viable alternative, as they convert the kinetic energy of river currents into electricity without requiring dams or diversion channels, reducing costs and minimizing environmental impact.

1.1. Energy context and rural challenges

Unequal access to electricity limits human development, education, and health in rural communities. In Colombia, the CREG [1] and UPME [3] point out that conventional electrification in dispersed areas involves high costs and low economic viability, which is why autonomous hybrid systems (solar, hydraulic, and wind) are emerging as an alternative for Non-Interconnected Zones (ZNI). Their implementation requires modular, economical, and low-maintenance solutions adapted to local conditions. In Colombia, recent studies on distributed generation through photovoltaic self-consumption systems demonstrate the feasibility of integrating renewable sources in urban and rural environments, supporting the transition to decentralized energy schemes [4].

The use of small-scale hydraulic energy is viable due to the abundance of rivers and streams. According to the Hydrological Atlas of Colombia [2] and the IDEAM Flow Measurement Manual [5], typical flows have velocities between 0.3 and 2.5 m/s, a range suitable for operating hydrokinetic microturbines if design and channeling are optimized.

1.2. Justification for the study

The project was carried out in the village of La Judía, municipality of Floridablanca, department of Santander (Colombia), located at 7.09° N and –73.05° W, at an altitude of approximately 1,200 meters above sea level. This rural area in the Andean foothills is characterized by small, low-flow rivers used for irrigation and local water supply.

The initiative arose from the need to implement a renewable energy source that would meet the basic electricity demand in a rural educational institution, with the aim of offering a sustainable and replicable alternative for the community. The low-flow watercourses that cross the area, which are not yet used for energy production, constitute an ideal natural laboratory for experimentation and technology demonstration.

The objective was to design, build, and validate a functional prototype of a hydraulic microturbine capable of operating in real river conditions, prioritizing affordable materials and low-cost manufacturing techniques, such as 3D printing. The research sought not only to demonstrate the technical feasibility of the system, but also its potential as an educational tool in the field of renewable energy training and community technology appropriation.

1.3. State of the art of hydrokinetic microturbines

Hydrokinetic systems use axial or transverse rotors immersed in river currents. Among the most studied configurations are the Darrieus, Savonius, and Gorlov rotors, which operate on the principle of aerodynamic lift [6]. The Gorlov-type rotor (GHT – Gorlov Helical Turbine) is characterized by its helical geometry, which allows continuous flow over the blades, reducing torque pulsation and improving efficiency at low speeds.

The general equation for power available in a velocity flow (v) is expressed as:

$$P_h = \frac{1}{2}\rho A\, v^3 \qquad (1)$$

Where ρ is the density of water (≈1000 kg/m³) and (A) is the area swept by the rotor. The theoretical Betz limit states that no turbine can capture more than 59.3% of this power [7]. In practice, the power coefficients C_p measured for laboratory turbines range from 0.1 to 0.35, depending on the geometry, number of blades, aspect ratio, and flow turbulence.

Several studies have addressed the development and evaluation of hydrokinetic microturbines with consistent experimental results. Espina-Valdés et al. [8] conducted an experimental comparison between Gorlov and Darrieus rotor configurations in low-speed flows (< 1 m/s), obtaining power coefficients C_p close to 0.25. Ferraiuolo et al. [9] analyzed the performance of a 3D-printed hydrokinetic turbine, demonstrating that the geometric adjustment of the blades and the alignment of the flow can increase operational efficiency. In the Colombian context, Pineda-Ortiz [10] developed a numerical model for Darrieus/Helical vertical axis turbines, highlighting the effect of aspect ratio and mechanical losses on overall performance. These studies agree that friction losses, flow misalignment, and inefficient coupling with the generator are the main limitations

to achieving greater efficiencies in small-scale prototypes.

Over the last decade, the international trend has been towards the application of additive manufacturing (3D printing) for the rapid and low-cost development of experimental hydrokinetic turbines. Recent studies have shown that this technology allows the rotor geometry to be adjusted to local flow conditions, reduces prototyping times, and decentralizes production, which is key for rural environments. Ferraiuolo et al. [9] characterized a 3D-printed horizontal turbine operating in low-velocity channels, while Rouway et al. [11] compared SLS (Selective Laser Sintering) and FFF (Fused Filament Fabrication) methods in reinforced polymer blades (Polyamide 12 - PA12), demonstrating structural and performance improvements. Similarly, Rengifo et al. [12] optimized an Archimedes spiral turbine made of PLA, and Armañanzas et al. [13] validated a closed-pipe turbine model using 3D printing. These advances confirm that additive manufacturing is establishing itself as a viable tool for decentralized hydrokinetic power generation, although challenges remain in terms of erosion resistance, geometric precision, and material certification, which this study addresses in the context of rural Colombia.

1.4. Contribution of this research

This study provides a comprehensive and experimental implementation in real conditions, integrating aerodynamic simulation, digital manufacturing, and hydraulic evaluation in the field. A NACA 0015 profile was chosen for its symmetry and angular stability in bidirectional flows. The combination of parametric CAD design, simulations in QBlade, and additive manufacturing allowed for rapid iteration between modeling and experimental testing.

Unlike previous work focused exclusively on laboratory environments, this prototype was installed directly in the natural channel, evaluating the effects of partial flow channeling through a 2.5 m long, 0.2 m diameter pipe. This allowed analysis of how channel geometry and local fluid acceleration influence the actual power coefficient and rotational stability.

1.5. Formulation of the problem and research question

The research focuses on the question: What design and construction parameters does a prototype hydraulic microturbine need in order to be used as an alternative energy source in rivers with modest flow rates? To answer this question, five specific and sequential objectives were defined: first, to hydraulically characterize the selected riverbed in the village of La Judía; second, to design a Gorlov rotor optimized for speeds below 0.5 m/s; third, to manufacture the prototype using 3D printing and modular assembly; fourth, to experimentally evaluate the overall efficiency of the system under two scenarios (free flow and channeled flow); and finally, to analyze the results obtained against the theoretical limit of Betz and comparable research in the area.

1.6. Environmental and educational relevance

The use of low-power hydrokinetic technologies not only contributes to reducing emissions, but also promotes an active learning model in rural communities. The installation of the prototype in a local educational institution allowed for the integration of applied science with environmental awareness, demonstrating how a natural resource can be transformed into clean energy in a tangible way.

Similarly, the simplicity of construction and accessibility of the material, mainly 3D-printed PETG and industrial PVC, facilitate its replicability in low-resource environments. Its low environmental impact, as it does not require damming or alterations to the riverbed, reinforces the compatibility of this type of technology with the Sustainable Development Goals (SDGs), especially SDG 7 (Affordable and clean energy) and SDG 13 (Climate action).

2. METHODOLOGY

The methodology used in the development of the hydraulic microturbine prototype was structured in five main phases: (1) hydraulic characterization of the river, (2) aerodynamic design and calculation of rotor parameters, (3) manufacturing and assembly of the system, (4) experimental implementation in the field, and (5) data processing and analysis. The entire process is summarized in Figure 1, which illustrates the stages followed from the initial characterization of the environment to the validation of the prototype.

The methodological approach adopted was experimental and analytical, based on the principles of hydraulic engineering, fluid mechanics, and computer-aided design (CAD), ensuring

consistency between numerical results, observed physical behavior, and actual operating conditions.

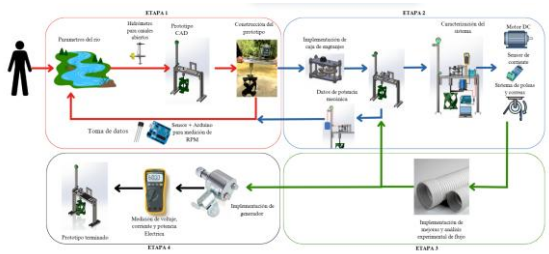

Fig. 1. *Stages followed from the initial characterization of the environment to the validation of the prototype.*
Source: *own elaboration.*

2.1. Hydraulic characterization of the site

The study was carried out in the village of La Judía, municipality of Floridablanca (Santander), selected for its permanent flow with an average velocity of 0.38 m/s and an approximate flow rate of 0.49 m³/s. The measurements were taken using a SEBA F1 current meter, applying the Ven Te Chow method [14], which considers the velocity at 0.6 of the total depth to estimate the representative average flow. The calculation of the available hydraulic power was based on the kinetic energy equation of the flow, suitable for free-flow systems without waterfall. In this way, the actual average power of the river under natural conditions is obtained:

$$P_h = \frac{1}{2}\rho A v^3 \rightarrow P_h = 37.33\ \text{W} \qquad (2)$$

Where $\rho = 997\ kg/m^3$, A = 1.3125 m^2 and $v = 0.38\ m/s$.

Likewise, the theoretical maximum power was calculated according to the Betz limit (59.3%) [7], obtaining a value that constitutes the upper physical threshold for any hydrokinetic conversion without losses.

$$P_{Betz} = 0.593 \text{ x } P_h \rightarrow P_{Betz} = 22.14\ \text{W} \qquad (3)$$

2.2. Aerodynamic design of the rotor

2.2.1. Selection of profile and geometric parameters

The rotor was designed with a Gorlov Helical Turbine (GHT) configuration, using three helical blades with a NACA 0015 profile. This profile was chosen for its symmetry, stability, and low drag coefficient in laminar flow conditions. The final design parameters are detailed in Table 1, while the CAD design of the Gorlov-type rotor, developed in SolidWorks, is shown in Figure 2.

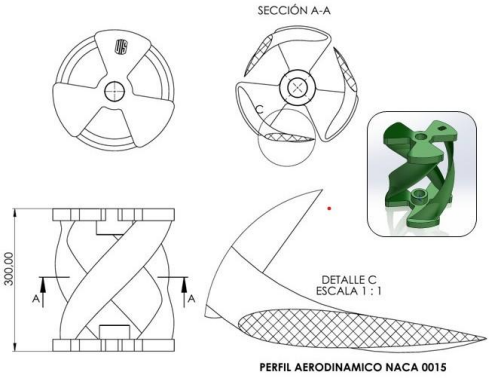

Fig. 2. *CAD design of the Gorlov-type rotor (NACA 0015) with helical pitch.*
Source: *own elaboration.*

Table 1. *Geometric characteristics of the rotor*

Parameter	Value	Unit
Diameter	0.25	m
Height	0.30	m
Angle of attack	14.5	°
Helical pitch angle	48.9	°
Chord	0.105	m
Number of blades	3	
Material	PETG (3D printing)	

Source: *own elaboration.*

2.2.2. Reynolds number

The Reynolds number (Re), calculated using the values shown below, allowed us to determine that the predominant low-turbulence regime, which is characteristic of natural flows in shallow rivers.

$\rho = 997\ kg/m^3,\ U = 0.38\ m/s,\ \text{L}_c = 0.105\ m,$ $\mu = 1.002 \text{ x } 10^3\ Pa - s$

$$Re = \frac{\rho U\, \text{L}_c}{\mu} \rightarrow Re \approx 39900 \qquad (4)$$

2.2.3. Tip Speed Ratio (TSR)

The Tip Speed Ratio (λ) was determined as follows:

$$\lambda = \frac{\omega R}{v} \qquad (5)$$

where ω is the angular velocity (rad/s), R = 0.125 m and $v = 0.38\ m/s$.

Under test conditions, 130 RPM (channeled flow) was recorded, equivalent to ω=13.61 rad/s. Substituting:

$$\lambda = \frac{13.61 \text{ x } 0.25}{0.38} \rightarrow \ \lambda = 4.47$$

This value is within the optimal range ($3 \leq \lambda \leq 5$) for Gorlov-type rotors, ensuring stability and good dynamic response.

2.2.4. Rotor solidity

Strength (σ) expresses the ratio between the total area of the blades and the area swept by the rotor. Based on the values $n = 3$, $C = 0.105$ m and $D = 0.25$ m, a value of $\sigma = 0.4$ was obtained. This level of solidity is considered moderate, as it provides an adequate balance between the starting torque and the aerodynamic efficiency of the Gorlov-type rotor.

$$\sigma = \frac{n\,C}{\pi D} \rightarrow \sigma = \frac{3 \text{ x } 0.105}{\pi \text{x } 0.25} \rightarrow \ \sigma = 0.40 \qquad (6)$$

2.3. Manufacturing and assembly

The prototype was manufactured using FDM 3D printing with high-strength PETG filament, with a density of 1.27 g/cm³, an extrusion temperature of 240 °C, and a layer height of 0.2 mm. The parts were then treated with epoxy putty and waterproof paint to improve surface strength.

The modular design allowed for easy transport and assembly in the field, as well as quick replacement of components in case of failure. The final assembly (see Fig. 3) integrated:

- ✓ A 0.25 m diameter helical rotor.
- ✓ A 1:12 gearbox made of PETG.
- ✓ 12 V, 6 W AC generator, dynamo type.
- ✓ Support structure in AISI 304 stainless steel, with 4.5 mm thick reinforcements.
- ✓ AISI 304 steel main shaft Ø10 mm, with sealed bearings for water.

Fig. 3. *Manufactured module, 3D-printed rotor, and free-flow testing (without channeling)*
Source: *own elaboration.*

2.4. Experimental implementation

The tests were carried out in the natural channel under two configurations:

- ✓ Free flow, i.e., without channeling (see Fig. 3).
- ✓ Channeled flow through a 2.5 m long, 15-inch diameter PVC pipe, which concentrated the flow, reducing lateral losses (see Fig. 4).

The experimental data, averaged from 30 consecutive measurements to minimize statistical dispersion, included the recording of the flow velocity both upstream and downstream, the RPM of the rotor measured with an optical tachometer, the voltage and output current of the generator (using a digital meter), and the temperature and environmental conditions. When comparing the results, it was found that the average RPM with channeling was 129.8, exceeding the 114 RPM obtained without channeling, which means a 13.9% increase in angular velocity.

Fig. 4. *Tests with PVC pipe channeling for flow stabilization.*
Fuente*: *Source: *own elaboration.*

2.5. Processing and efficiency analysis

The overall efficiency of the system(η_{total}) was determined by comparing the electrical power obtained with the available hydraulic power.

$$\eta_{total} = \frac{P_{electrica}}{P_h} \text{x } 100 \qquad (7)$$

Where $P_{electrica} = 3.3$ W and $P_h = 37.33$ W.
Therefore:

$$\eta_{total} = 8.84\%$$

This value is consistent with the experimental power coefficient $C_p = 0.088$, within the range reported for low-speed experimental microturbines.

To reinforce the reliability of the results, a qualitative analysis of measurement uncertainty was performed. The SEBA F1 windmill has an accuracy of ±2% in speed, while the digital multimeter

records voltage and current with an accuracy of ±0.5% and ±1%, respectively. The variation in water temperature (±1.5 °C), which slightly affects the density and viscosity of the fluid, was also considered. The combined effect of these sources of error is estimated to be less than 5% of the measured value, so it does not significantly alter the efficiency or the comparison between free and channeled flow.

2.6. Laboratory validation

Fig. 5. *Laboratory tests in a hydraulic flume.*
Source: *own elaboration.*

Additionally, the system was tested in the hydraulics laboratory at the Industrial University of Santander, using a test channel (see Fig. 5). However, the flow available in this channel was insufficient in depth and velocity to completely cover the rotor, which limited the possibility of performing a comprehensive validation under controlled conditions. Even so, the tests were valuable in verifying the structural rigidity, dynamic balance of the rotor, and mechanical coupling of the system, confirming the stability of the assembly during free rotation.

3. RESULTS AND DISCUSSION

The experimental evaluation of the prototype allowed us to characterize the behavior of the system under real operating conditions and compare the results obtained with the estimated theoretical values and with previous studies on small-scale hydrokinetic turbines. The analysis was structured in three complementary levels: first, the hydraulic and rotational performance of the rotor was examined; then, the energy efficiency and power generated were determined; and finally, a theoretical comparison was made to identify the factors limiting overall performance.

3.1. Hydraulic and rotational performance

The experimental tests were carried out in two different scenarios: in free flow, without channeling, and in channeled flow using a PVC pipe 2.5 m long and 15 inches in diameter. In both cases, the rotor's revolutions per minute (RPM) were recorded, with a notable increase in stability and rotation speed when the flow was channeled, due to the reduction in turbulence and lateral losses. Table 2 shows the average values obtained from the 30 repetitions carried out in the field, which reflect the dynamic behavior of the rotor under both test conditions.

Table 2. *Experimental results for angular velocity.*

Flow condition	Average RPM	ω (rad/s)	Variation (%)
Free flow	114.2	11.94	—
Channeled flow	129.8	13.61	+13.9

Source: *own elaboration.*

It was observed that the pipe not only increased the angular velocity but also significantly reduced the RPM fluctuation between consecutive measurements. This behavior is attributed to a decrease in the transverse velocity gradient and the development of a more uniform flow in the inlet section, as proposed by flow channeling studies in hydrokinetic turbines [14]. In addition, the partial Venturi effect induced by the reduction in section generated an acceleration of the fluid downstream, which increased the local Reynolds number and favored the turbulent regime desired for stable rotor operation.

3.2. Electrical power generated

The output voltage of the alternating current (AC) generator was recorded at 10-second intervals using a digital multimeter. Under channeled flow conditions, the average values obtained were V=2.9 V and I=1.14 A, corresponding to an effective electrical power of 3.3 W. This result is significant considering the small dimensions of the rotor (0.25 m in diameter) and the low flow velocity (0.38 m/s). In contrast, under free flow conditions, the average power achieved was 2.1 W, showing a 57% increase when channeling the flow, associated with better kinetic energy concentration and a decrease in local turbulence.

3.3. Overall hydraulic efficiency

The overall efficiency of the system was calculated using the ratio between the electrical power obtained

and the available hydraulic power (Equation 7). The results are summarized in Table 3.

Table 3. *System efficiency under different configurations*

Condition	Hydraulic power (W)	Electrical power (W)	Total efficiency (%)
Free flow	37.33	2.1	5.6
Channeled flow	37.33	3.3	8.8

Source: *own elaboration.*

The experimental power coefficient C_p obtained for the prototype reached a maximum value of 0.088 under channeled flow conditions, which is equivalent to an overall efficiency of 8.8%. The value obtained is within the expected ranges for small-scale hydrokinetic microturbines, which supports the validity of the design and the consistency of the experimental measurements. Although the efficiency is modest compared to the theoretical Betz limit $C_{p,\text{Betz}} = 0.593$, this difference is explained by the mechanical and electrical losses of the system, the low Reynolds number (≈ 39 900), and the limited flow velocity (0.38 m/s), factors that restrict momentum transfer and lift generation on the blades. At higher flow velocities (> 0.6 m/s), a proportional increase in C_p and power generated would be expected, suggesting significant room for improvement for future geometric and operational optimizations of the rotor.

3.4. $C_p - \lambda$ ratio

The aerodynamic behavior of the rotor was analyzed based on the relationship between the power coefficient C_p and the tip speed ratio (λ), a fundamental parameter for evaluating energy conversion efficiency in hydrokinetic turbines.

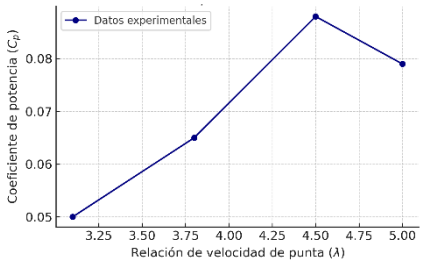

Fig. 6. *Experimental curve of the $C_p - \lambda$ relationship for the Gorlov-type rotor.*
Source: *own elaboration.*

The experimental values obtained (Table 5) show a progressive increase in C_p until reaching a maximum of $C_p = 0.088 = 0.088$ for $\lambda_{opt} = 4.5$ (see Fig. 6), in line with the typical trend for lift turbines. This behavior coincides with the numerical predictions obtained through simulations in QBlade, which validates the geometric design of the rotor and the selection of the NACA 0015 profile.

Table 5 shows the experimental values obtained for different tip speed ratios. It shows the point of maximum aerodynamic performance followed by a progressive decrease associated with increased drag and separation losses, which is characteristic behavior in vertical axis lift rotors.

Table 5. *Experimental $C_p - \lambda$ ratio*

λ	C_p
3.1	0.050
3.8	0.065
4.5	0.088
5.0	0.079

Source: *own elaboration.*

3.5. Influence of piping and system losses

Piping had a direct effect on flow stability, reducing the level of transverse turbulence and improving the uniformity of the velocity field. This was reflected in an increase in RPM and C_p, but also introduced new friction losses on the pipe wall, which were estimated using the Darcy-Weisbach equation:

$$h_f = f\frac{L}{D}\frac{v^2}{2g} \qquad (8)$$

where f = 0.03, L = 2.5 m, D = 0.381 m, v = 0.38 m/s, and g=9.81 m/s^2.

The result was $h_f = 0.0114\ m$, an insignificant loss compared to the hydraulic benefit obtained.

On the other hand, the mechanical coupling between the shaft and the generator presented power losses of around 15%, mainly due to friction in bearings and angular play in 3D-printed gears. These losses could be reduced by precision CNC machining, sealed lubrication, and optical alignment of the transmission system.

3.6. Comparison with other studies

The results obtained were compared with recent research on low-speed hydrokinetic microturbines published between 2019 and 2025. In general, these studies agree that conversion efficiency C_p depends

mainly on the incident flow velocity, the degree of hydraulic confinement, and the rotor geometry.

Yosry et al. experimentally analyzed a small-scale vertical axis turbine using VOF-3D simulations considering the variation of the free surface of the channel, demonstrating that hydraulic blockage can increase C_p by up to 20% compared to free flow [15]. Complementarily, Espina-Valdés et al. compared the Gorlov and Darrieus configurations in a hydrodynamic tunnel, finding greater stability and torque in the helical rotor, although they noted an overestimation of C_p in confined channels [8].

Taking a different methodological approach, Abed et al. developed an efficient hydrodynamic model to predict the performance of cross-flow turbines, validated experimentally at speeds between 0.43 and 0.73 m/s, showing a high degree of agreement with numerical results [16]. For their part, Tunio et al. evaluated the effect of booster nozzles on Darrieus turbines, verifying that these can double the power generated, albeit at the cost of greater structural efforts [17].

More recently, Pineda et al. optimized a 3D-printed Gorlov turbine for river applications in the laboratory using the response surface methodology, achieving a C_p of 0.10 under low-speed conditions (0.45 m/s) [18]. Similarly, Chica et al. evaluated a full-scale horizontal-axis hydrokinetic turbine for rural applications in Colombia, achieving a C_p of 0.09 and highlighting the viability of distributed generation solutions in developing countries [19].

Comparatively, the prototype developed in this study presented a $C_p = 0.088$ under channeled flow, a value consistent with the reported ranges (0,05–0,12) for low-speed, unconstrained experimental systems. This result supports the validity of the approach adopted, demonstrating the technical and social relevance of low-cost, low-environmental-impact, and highly reproducible hydrokinetic solutions for rural environments.

3.7. Social and educational implications

The prototype demonstrated its potential as an educational tool by facilitating practical understanding of the conversion of hydraulic energy into electrical energy in rural schools. Its low cost, local manufacturing, and environmentally friendly operation make it an appropriate technology for rural communities. Thanks to its modularity and easy maintenance, it can be integrated into decentralized energy programs and community technical training. These types of devices can be incorporated into experimental microgrid schemes and educational laboratories, such as those proposed by Santos-Montes et al. [20], promoting practical teaching of energy conversion and management.

Low-cost technological initiatives aimed at environmental and energy education, such as the automation of anaerobic digesters for biogas production developed in the country [21], reinforce the role of local innovation as a pedagogical tool for rural sustainability.

3.8. Limitations of the study

The main limitation of this study lies in the low flow velocity (≈ 0.38 m/s), which restricted the power that could be generated and, consequently, the overall efficiency of the system. Future evaluations are recommended in scenarios with velocities between 0.6 and 0.8 m/s, where the power coefficient C_p could be significantly increased.

On the other hand, the geometric accuracy of the blades manufactured using fused deposition modeling (FDM) 3D printing showed small deviations in the aerodynamic profile and twist angle, slightly affecting the lift distribution and dynamic balance of the rotor. These imperfections can be mitigated by using higher resolution printers, stable thermal control, fine extruder calibration, and surface smoothing post-processes that improve finish quality and reduce edge irregularities.

Finally, the AC generator used was not designed for low revolutions, which limited the total electromechanical conversion. Future iterations should incorporate multipole alternators or low-speed permanent magnet generators (PMSG), which are more suitable for hydrokinetic applications.

4. CONCLUSIONS

The development and experimental evaluation of the Gorlov-type hydraulic microturbine demonstrated the technical and operational feasibility of harnessing the kinetic energy of low-flow river currents in rural Colombian environments. The system, designed using aerodynamic criteria and manufactured using additive manufacturing, showed stable, reproducible performance consistent with the efficiency values reported in recent literature.

Likewise, the experience in La Judía validated the principle that river energy can be transformed into

useful electricity using simple, sustainable, and low-cost devices, without requiring large infrastructures. This approach consolidates a model of applied engineering and technological education, where innovation arises from local contextualization, creativity, and practical knowledge. In the future, it is planned to scale up the rotor design and evaluate its integration into hybrid rural microgrids, where it can be complemented by solar or wind sources to improve the reliability of energy supply in non-interconnected communities. Consequently, small-scale hydrokinetic microturbines are emerging as a strategic tool for a fair and decentralized energy transition in Colombia and Latin America. As Palma et al. [22] point out, the adoption of renewable solutions and energy efficiency measures in public institutions represents a key strategy for advancing toward national energy sustainability, consistent with the results obtained in this study.

REFERENCES

[1] Comisión de Regulación de Energía y Gas (CREG), Documento de Soporte Resolución 093 de 2011 – Zonas No Interconectadas, Bogotá D.C., Colombia, 2011.

[2] Unidad de Planeación Minero Energética (UPME), Atlas Hidrológico de Colombia, Bogotá D.C., Colombia, 2020.

[3] Unidad de Planeación Minero Energética (UPME), Plan Energético Nacional 2020–2050, Bogotá D.C., Colombia, 2021.

[4] F. A. Lara Vargas, M. Á. Ortiz Padilla y C. A. Vargas Salgado, "Análisis experimental comparativo de la producción anual de energía de una planta solar fotovoltaica de 72 kW_n instalada sobre techo para autoconsumo en la ciudad de Montería utilizando PVsyst, PVGIS y SAM," Revista Colombiana de Tecnologías de Avanzada (RCTA), vol. 1, no. 43, pp. 51–56, 2024.

[5] Instituto de Hidrología, Meteorología y Estudios Ambientales (IDEAM), Manual para la Medición de Caudales en Corrientes Superficiales, Bogotá D.C., Colombia, 2018.

[6] I. Gorlov, "Helical Turbine and Fish Friendly Hydropower Generation Method," U.S. Patent 5,451,137, 1995.

[7] A. Betz, Wind-Energie und ihre Ausnutzung durch Windmühlen, Göttingen: Vandenhoeck & Ruprecht, 1926.

[8] R. Espina-Valdés, R. Ferraiuolo, A. Fernández-Jiménez, G. Del Giudice, E. Álvarez-Álvarez y M. Giugni, "Experimental comparison between hydrokinetic turbines: Assessment of Gorlov and Darrieus configurations in low-velocity flows," Energies, vol. 15, no. 13, p. 4726, 2022. doi: 10.3390/en15134726.

[9] R. Ferraiuolo, A. Gharib-Yosry, A. Fernández-Jiménez, R. Espina-Valdés, E. Álvarez-Álvarez, G. Del Giudice y M. Giugni, "Design and experimental performance characterization of a three-blade horizontal-axis hydrokinetic water turbine in a low-velocity channel," Environmental Sciences Proceedings, vol. 21, no. 1, art. 62, 2022. doi: 10.3390/environsciproc2022021062.

[10] J. C. Pineda-Ortiz, "Métodos numéricos para el desarrollo de una turbina hidrocinética de eje vertical tipo Darrieus/Helicoidal," Revista UIS Ingenierías, vol. 19, no. 1, pp. 78–94, 2020. [En línea]. Disponible en: https://revistas.uis.edu.co/index.php/revistauisingenierias/article/view/10731

[11] M. Rouway, M. Nachtane, M. Tarfaoui y S. Jamoudi Sbai, "3D printing of a tidal turbine blade using two methods of SLS and FFF of a reinforced PA12 composite: A comparative study," Sustainable Marine Structures, vol. 6, no. 1, pp. 1–19, Mar. 2024. doi: 10.36956/sms.v6i1.1002.

[12] J. Rengifo, L. Velásquez, E. Chica y A. Rubio-Clemente, "Optimization of the Archimedean spiral hydrokinetic turbine design using response surface methodology," Sci, vol. 7, no. 3, art. 100, 2025. doi: 10.3390/sci7030100.

[13] J. Armañanzas, M. Alcalá, J. P. Fuertes, J. León, A. Torres y M. Gil, "Design and optimization of LCA blade turbine for electrical energy generation in closed pipes," WSEAS Transactions on Fluid Mechanics, vol. 19, pp. 64–71, 2024. doi: 10.37394/232013.2024.19.7.

[14] V. T. Chow, Open Channel Hydraulics, New York, NY, USA: McGraw-Hill, 1959.

[15] A. G. Yosry, E. Á. Álvarez, R. Espina-Valdés, A. Pandal y E. B. Marigorta, "Experimental and multiphase modeling of small vertical-axis hydrokinetic turbine with free-surface variations," Renewable Energy, vol. 203, pp. 788–801, 2023. doi: 10.1016/j.renene.2022.12.114.

[16] B. Abed et al., "An efficient hydrodynamic method for cross-flow turbines performance evaluation and comparison with the experiment," Renewable Energy, vol. 180, pp. 993–1003, 2021. doi: 10.1016/j.renene.2021.09.004.

[17] I. A. Tunio et al., "Investigation of duct-augmented system effect on the overall performance of straight-blade Darrieus hydrokinetic turbine," Renewable Energy, vol.

153, pp. 143–154, 2020. doi: 10.1016/j.renene.2020.02.012.

[18] J. C. Pineda, A. Rubio-Clemente y E. Chica, "Optimization of a Gorlov helical turbine for hydrokinetic application using the response surface methodology and experimental tests," Energies, vol. 17, no. 22, p. 5747, 2024. doi: 10.3390/en17225747.

[19] E. Chica, L. Velásquez y A. Rubio-Clemente, "Full-scale experimental assessment of a horizontal-axis hydrokinetic turbine for river applications: A challenge for developing countries," Energies, vol. 18, no. 7, p. 1657, 2025. doi: 10.3390/en18071657.

[20] A. J. Santos-Montes, D. F. Duarte, C. J. Gómez y J. C. Pérez, "Laboratory prototype for testing electrical devices and emulating real microgrids," Revista Colombiana de Tecnologías de Avanzada (RCTA), vol. 1, no. 45, pp. 216–224, 2025. doi: 10.24054/rcta.v1i45.3477.

[21] C. A. V. Herrera, J. A. Sánchez, J. A. Cely y D. A. Arévalo, "Automatización de un digestor anaerobio con sistema embebido para la producción de biogás a partir de residuo del aceite de palma," Revista Colombiana de Tecnologías de Avanzada (RCTA), vol. 2, no. 44, pp. 25–34, 2024.

[22] H. H. Palma, D. J. Novoa y D. Mendoza Cásseres, "Energías renovables y medidas de eficiencia energética aplicables a las instituciones prestadoras de salud en Colombia," Revista Colombiana de Tecnologías de Avanzada (RCTA), vol. 1, no. 41, pp. 123–131, 2023.